

A sensitivity study of artificial viscosity in a defect-deferred correction method for the coupled Stokes/Darcy model

YANAN YANG AND PENGZHAN HUANG*

*College of Mathematics and System Sciences, Xinjiang University, Urumqi 830 017,
P. R. China*

Received September 9, 2021; accepted May 25, 2022

Abstract. This paper analyzes the sensitivity of artificial viscosity in the defect-deferred correction method for the non-stationary coupled Stokes/Darcy model. For the defect step and the deferred-correction step of the defect deferred correction method, we give the corresponding sensitivity systems related to the change of artificial viscosity. Finite element schemes are devised for computing numerical solutions to the sensitivity systems. Finally, we verify the theoretical analysis results through numerical experiments. The paper shows the effects of artificial viscosity, viscosity/hydraulic conductivity coefficients and spatial step sizes on sensitivity of numerical solutions to artificial viscosity in the defect step and the deferred correction step in detail.

AMS subject classifications: 65M60

Keywords: artificial viscosity, sensitivity systems, defect-deferred correction method, Stokes/Darcy model

1. Introduction

In recent years, the coupled Stokes/Darcy model and the coupled Navier-Stokes/Darcy model have received more and more attention in science and engineering, especially in cases where a free flowing fluid moves over a porous medium, such as the soil pollution problem, oil drilling simulation, filtering surface water and blood motion in the vessels, etc. [19, 24]. In such regions, compared with the Stokes equations, the Navier-Stokes equations can more accurately describe the flow of liquids in cavities and conduits. Since fluids often flow relatively slowly, we can simplify the nonlinear Navier-Stokes equations into the linear Stokes equations. In this paper, we mainly focus on the coupled Stokes/Darcy model which consists of the Stokes equations and Darcy's law to control the free flow and the porous media flow respectively, and then couples them together through some interface conditions between two subdomains. Obviously, it is of great significance to develop some effective numerical methods to investigate the Stokes/Darcy model.

The Stokes/Darcy model has different governing equations in different regions and possesses multiple physical quantities which have caused various difficulties and problems in the numerical simulation of the model. To overcome the complexity

*Corresponding author. *Email addresses:* yangyn996@sina.com (Y. Yang), hpzh@xju.edu.cn (P. Huang)

of this model, many numerical methods for solving the Stokes/Darcy system have been proposed. For example, aiming at the mathematical difficulties in coupled multiphysical model simulation for the steady state problem, Cai et al. proposed in [8] a decoupled and linearized two-grid algorithm. In order to improve the accuracy of numerical solutions and achieve mass conservation in the finite element method for non-stationary problem, the rotational form of the pressure-correction method was presented by Li et al. in [21]. Qin and Hou have added a time filter to the backward Euler scheme of the Stokes/Darcy model to increase the accuracy of the time from the first order to the second order [27]. There are also discontinuous Galerkin methods [29], interface relaxation methods [4] and decoupled methods based on two-grid or multi-grid finite elements [23, 7, 12], and other works presented in [31, 10, 18, 22] and the references therein.

The defect-deferred correction method was used by Aggul, Connors, Erkmén, and Labovsky when solving the problem of fluid-fluid interaction [2]. For this method, it can deal with the problem with small parameters. The defect step uses a simple and effective artificial viscosity to increase the viscosity coefficient of the flow. After that, a deferred correction step is established and applied to the data-passing scheme [13, 11] to create an unconditionally stable second-order precision partition time. Currently, the defect-deferred correction method is successfully tested in the application to the one-domain Navier-Stokes equations [3] and the two-domain convection dominated convection diffusion problem [13].

In the solution of many fluid problems, very fine meshes are often required, which results in expensive costs of each calculation. Therefore, the influence of a different selection of artificial parameters on the numerical solution of the equation is very important. On the other hand, studying the sensitivity of physical quantities to parameters in fluid problems is of great significance for a more comprehensive analysis of flow behavior and understanding of the reliability of numerical solutions [1, 5, 14, 26, 32]. The common method for calculating sensitivity is the continuous sensitivity equation method [6]. Firstly, the sensitivity equations are derived by differentiating with a dependent variable or parameter in original continuum equations. Secondly, after solving the numerical solution of the original equation, the sensitivity of the numerical solution to the parameters is obtained by solving linear equations derived from sensitive equations. Since the continuous sensitivity equation method has the advantage of avoiding a delicate issue of computing mesh sensitivities and the issue of differentiating computational facilitators, more and more works are focused on the continuous sensitivity equation method [5, 14, 20, 25, 32]. Li and Huang have studied sensitivity analysis of the relaxation parameter in the Uzawa algorithm for the steady natural convection model [20]. Neda et al. have discussed sensitivity analysis of the grad-div stabilization parameter in finite element simulations of incompressible flow [25].

In this paper, we use the continuous sensitivity equation method to study the sensitivity of artificial viscosity of the defect-deferred correction method for the coupled Stokes/Darcy problem. These sensitivity equations are developed by taking a derivative of the defect-deferred correction method of the non-stationary coupled Stokes/Darcy model with respect to artificial viscosity. Besides, the solutions to the sensitivity equations can be used to estimate the reliability of the non-stationary

coupled Stokes/Darcy model in terms of artificial viscosity in the defect-deferred correction method.

2. Coupled Stokes/Darcy model

Let us take into account the model for coupling fluid and porous media flows in a bound smooth domain $\Omega \subset \mathbb{R}^2$, which consists of two sub-domains Ω_f and Ω_p . Interface Γ divides Ω into Ω_p and Ω_f , i.e. $\Omega = \Omega_p \cup \Omega_f$. Next, boundary $\Gamma_f = \partial\Omega_f \cap \partial\Omega$, $\Gamma_p = \partial\Omega_p \cap \partial\Omega$ and interface $\Gamma = \partial\Omega_f \cap \partial\Omega_p$ are introduced. In the rest of this paper, we always use boldface characters to denote vectors or vector spaces. \mathbf{n}_p and \mathbf{n}_f represent the unit outward normal vector of $\partial\Omega_p$ and the unit outward normal vector of $\partial\Omega_f$, respectively. The motion in fluid region Ω_f is governed by the Stokes equations [27, 28]:

$$\begin{aligned} \frac{\partial \mathbf{u}_f}{\partial t} - \nabla \cdot (\mathbb{T}_\nu(\mathbf{u}_f, p_f)) &= \mathbf{g}_f, & \text{in } \Omega_f, \\ \nabla \cdot \mathbf{u}_f &= 0, & \text{in } \Omega_f, \\ \mathbf{u}_f(\mathbf{x}, 0) &= \mathbf{u}_f^0(\mathbf{x}), & \text{in } \Omega_f, \end{aligned} \quad (1)$$

where $\mathbb{T}_\nu(\mathbf{u}_f, p_f) = -p_f \mathbb{I} + 2\nu \mathbb{D}(\mathbf{u}_f)$ is the stress tensor and $\mathbb{D}(\mathbf{u}_f) = \frac{1}{2}(\nabla \mathbf{u}_f + \nabla^T \mathbf{u}_f)$ is the deformation rate tensor. \mathbb{I} is the identity tensor expressed as:

$$\mathbb{I} = \begin{bmatrix} 1 & 0 \\ 0 & 1 \end{bmatrix}.$$

ν is the kinematic viscosity and $\mathbf{g}_f(\mathbf{x}, t)$ is the external force. The motion in porous medium region Ω_p is governed by

$$\begin{aligned} \frac{S_0 \partial \phi_p}{\partial t} - \nabla \cdot \mathbb{K} \nabla \phi_p &= g_p, & \text{in } \Omega_p, \\ \phi_p(\mathbf{x}, 0) &= \phi_p^0(\mathbf{x}), & \text{in } \Omega_p, \end{aligned} \quad (2)$$

where S_0 is the water storage coefficient. \mathbb{K} represents the hydraulic conductivity in Ω_p , which is the positive symmetric tensor, allowed to change in space. The $g_p(\mathbf{x}, t)$ is a source term with a solvability condition $\int_{\Omega_p} g_p(\mathbf{x}, t) = 0$. The above equations (1) and (2) are coupled together by the following boundary conditions:

$$\mathbf{u}_f = 0, \quad \text{on } \Gamma_f, \quad \phi_p = 0, \quad \text{on } \Gamma_p,$$

and the interface conditions on Γ :

$$\begin{aligned} \mathbf{u}_f \cdot \mathbf{n}_f - \mathbb{K} \nabla \phi_p \cdot \mathbf{n}_p &= 0, \\ -[\mathbb{T}_\nu(\mathbf{u}_f, p_f) \cdot \mathbf{n}_f] \cdot \mathbf{n}_f &= g \phi_p, \\ -[\mathbb{T}_\nu(\mathbf{u}_f, p_f) \cdot \mathbf{n}_f] \cdot \boldsymbol{\tau} &= \frac{\sqrt{2\alpha\nu}}{\sqrt{\text{trace} \mathbb{I}}} \mathbf{u}_f \cdot \boldsymbol{\tau}, \end{aligned}$$

where $\boldsymbol{\tau}$ is the orthogonal tangential unit vector along Γ . α is an experimentally validated parameter and $\boldsymbol{\Pi}$ represents the permeability. Here g represents the gravitational constant. This interface condition is called the Beavers-Joseph-Saffman interface condition [30, 17, 9, 16].

Then, let us introduce some function spaces:

$$\begin{aligned} \mathbf{X}_f &= \{\mathbf{v}_f \in \mathbf{H}^1(\Omega_f) : \mathbf{v}_f|_{\Gamma_f} = 0\}, & X_p &= \{\psi_p \in H^1(\Omega_p) : \psi_p|_{\Gamma_p} = 0\}, \\ Q_f &= L^2(\Omega_f), & \mathbf{U} &= \mathbf{X}_f \times X_p. \end{aligned}$$

We equip the domain D ($D = \Omega_p$ or Ω_f) with the usual L^2 -scalar product $(\cdot, \cdot)_D$ and L^2 -norm $\|\cdot\|_D$, which is expressed as $\|\cdot\|_{L^2}$. On the interface Γ , the L^2 inner product is defined as $(\cdot, \cdot)_\Gamma$. Besides, spaces \mathbf{X}_f and X_p are equipped with the following norms:

$$\begin{aligned} \|\mathbf{v}_f\|_f &= \|\nabla \mathbf{v}_f\|_{L^2} = \sqrt{(\nabla \mathbf{v}_f, \nabla \mathbf{v}_f)_{\Omega_f}}, & \forall \mathbf{v}_f \in \mathbf{X}_f, \\ \|\psi_p\|_p &= \|\nabla \psi_p\|_{L^2} = \sqrt{(\nabla \psi_p, \nabla \psi_p)_{\Omega_p}}, & \forall \psi_p \in X_p. \end{aligned}$$

The space \mathbf{U} is equipped with the norms: $\forall \underline{\mathbf{u}} = (\mathbf{u}_f, \phi_p)^T \in \mathbf{U}$,

$$\begin{aligned} \|\underline{\mathbf{u}}\|_0 &= \sqrt{(\mathbf{u}_f, \mathbf{u}_f)_{\Omega_f}} + \sqrt{gS_0(\phi_p, \phi_p)_{\Omega_p}}, \\ \|\underline{\mathbf{u}}\|_{\mathbf{U}} &= \sqrt{\nu(\nabla \mathbf{u}_f, \nabla \mathbf{u}_f)_{\Omega_f}} + \sqrt{g(\mathbb{K}\nabla \phi_p, \nabla \phi_p)_{\Omega_p}}. \end{aligned}$$

For functions $v(x, t)$, we define the norms:

$$\|v\|_{L^2(0, T; \mathbf{L}^2(\Omega))} = \left(\int_0^T \|v(\cdot, t)\|_{L^2}^2 dt \right)^{\frac{1}{2}}, \quad \|v\|_{L^\infty(0, T; \mathbf{L}^2(\Omega))} = \operatorname{ess\,sup}_{(0 < t < T)} \|v(\cdot, t)\|_{L^2}.$$

Then the variational formulation for the time-dependent Stokes/Darcy model is as follows: For $\mathbf{g}_f \in L^2(0, T; \mathbf{L}^2(\Omega_f))$ and $g_p \in L^2(0, T; L^2(\Omega_p))$, find $\underline{\mathbf{u}} = (\mathbf{u}_f, \phi_p)^T \in L^2(0, T; \mathbf{X}_f) \cap L^\infty(0, T; \mathbf{L}^2(\Omega_f)) \times L^2(0, T; X_p) \cap L^\infty(0, T; L^2(\Omega_p))$ and $p_f \in L^2(0, T; Q_f)$ such that $\forall (\mathbf{v}, q_f) \in \mathbf{U} \times Q_f$ satisfying

$$\begin{aligned} (\underline{\mathbf{u}}_t, \mathbf{v}) + a(\underline{\mathbf{u}}, \mathbf{v}) - b(\mathbf{v}, p_f) + b(\underline{\mathbf{u}}, q_f) &= \langle \mathbf{F}, \mathbf{v} \rangle_{\mathbf{U}'}, \\ \underline{\mathbf{u}}(\mathbf{x}, 0) &= \underline{\mathbf{u}}^0, \end{aligned}$$

where

$$\begin{aligned} (\underline{\mathbf{u}}_t, \mathbf{v}) &= (\mathbf{u}_{f,t}, \mathbf{v}_f)_{\Omega_f} + (S_0 \phi_{p,t}, \psi_p)_{\Omega_p}, & a(\underline{\mathbf{u}}, \mathbf{v}) &= a_\Omega(v \underline{\mathbf{u}}, \mathbf{v}) + a_\Gamma(\underline{\mathbf{u}}, \mathbf{v}), \\ a_\Omega(v \underline{\mathbf{u}}, \mathbf{v}) &= a_{\Omega_f}(\nu \mathbf{u}_f, \mathbf{v}_f) + a_{\Omega_p}(\mathbb{K} \phi_p, \psi_p), & a_{\Omega_p}(\mathbb{K} \phi_p, \psi_p) &= g(\mathbb{K} \nabla \phi_p, \nabla \psi_p)_{\Omega_p}, \\ a_{\Omega_f}(\nu \mathbf{u}_f, \mathbf{v}_f) &= 2\nu(\nabla \mathbf{u}_f, \nabla \mathbf{v}_f)_{\Omega_f} + \left(\frac{\alpha \sqrt{2}}{\sqrt{\operatorname{trace} \boldsymbol{\Pi}}} ((\mathbf{u}_f, \mathbf{v}_f) - ((\mathbf{u}_f, \mathbf{v}_f) \cdot \mathbf{n}_f) \mathbf{n}_f) \right)_\Gamma, \\ \langle \mathbf{F}, \mathbf{v} \rangle_{\mathbf{U}'} &= (\mathbf{g}_f, \mathbf{v}_f)_{\Omega_f} + g(g_p, \psi_p)_{\Omega_p}, & a_\Gamma(\underline{\mathbf{u}}, \mathbf{v}) &= g(\phi_p, \mathbf{v}_f \cdot \mathbf{n}_f)_\Gamma - g(\psi_p, \mathbf{u}_f \cdot \mathbf{n}_f)_\Gamma, \\ b(\mathbf{v}, p_f) &= (p_f, \nabla \cdot \mathbf{v}_f)_{\Omega_f}, \end{aligned}$$

where \mathbf{U}' is the dual space of \mathbf{U} . In particular, v does not have a specific physical meaning. It is only used to keep $a_\Omega(v\mathbf{u}, \mathbf{v})$ the same writing structure as $a_{\Omega_f}(\nu\mathbf{u}_f, \mathbf{v}_f)$ and $a_{\Omega_p}(\mathbb{K}\phi_p, \psi_p)$, so as to facilitate subsequent corrections with algorithms. The bilinear forms are continuous and coercive (refer to [10]). $\forall \mathbf{u}, \mathbf{v} \in \mathbf{U}$,

$$\begin{aligned} a(\mathbf{u}, \mathbf{v}) &\leq C_{con} \|\mathbf{u}\|_{\mathbf{U}} \|\mathbf{v}\|_{\mathbf{U}}, & a(\mathbf{u}, \mathbf{u}) &\geq C_{coe} \|\mathbf{u}\|_{\mathbf{U}}^2, \\ a_\Gamma(\mathbf{u}, \mathbf{v}) &\leq C_\Gamma \|\mathbf{u}\|_{\mathbf{U}} \|\mathbf{v}\|_{\mathbf{U}}, & \forall \mathbf{u}, \mathbf{v} &\in \mathbf{U}, \end{aligned}$$

where C_{con} , C_{coe} and C_Γ are positive constants and not dependent on the data of the problem. Additionally,

$$a_\Gamma(\mathbf{u}, \mathbf{v}) = -a_\Gamma(\mathbf{v}, \mathbf{u}) \quad \text{and} \quad a_\Gamma(\mathbf{u}, \mathbf{u}) = 0, \quad \forall \mathbf{u}, \mathbf{v} \in \mathbf{U}.$$

For the theoretical analysis, we introduce the trace and Poincaré inequalities. There exist positive constants C_p and \tilde{C}_p that depend on the domains Ω_f and Ω_p respectively, such that for all $\mathbf{v}_f \in \mathbf{X}_f$ and $\psi_p \in X_p$,

$$\|\mathbf{v}_f\|_{L^2} \leq C_p \|\mathbf{v}_f\|_f, \quad \|\psi_p\|_{L^2} \leq \tilde{C}_p \|\psi_p\|_p.$$

3. The defect-deferred correction method and the sensitivity equation

Firstly, let $\{t_n = n\Delta t\}_{n=0}^N$ be the mean of the time interval $[0, T]$, and the time step $\Delta t = \frac{T}{N}$. Secondly, τ_{fh} is constructed as regular triangles of Ω_f in a 2D domain with max diameter h_f . Further, for Ω_p , we also define τ_{ph} with max diameter h_p . Then $h = \max\{h_f, h_p\}$ is set as the maximum diameter of Ω . For simplicity, we assume that Ω_f and Ω_p are smooth domains. Let $\mathbf{X}_{fh} \subset \mathbf{X}_f$, $Q_{fh} \subset Q_f$, and $X_{ph} \subset X_p$ are finite element spaces. Furthermore, the finite element space pair $(\mathbf{X}_{fh}, Q_{fh})$ is assumed to satisfy the usual discrete inf-sup condition or the LBB condition for the stability of the discrete pressure:

$$\inf_{q_{fh} \in Q_{fh}} \sup_{\mathbf{v}_h \in \mathbf{X}_{fh}} \frac{b(\mathbf{v}_h, q_{fh})}{\|\mathbf{v}_h\|_{\mathbf{X}_f} \|q_{fh}\|_{Q_f}} \geq \beta > 0,$$

where β is a constant independent of h . In fact, many finite element space pairs satisfy the discrete inf-sup condition, such as Taylor-Hood elements (P2-P1, P3-P2) and the Scott-Vogelius element. In this paper, the theoretical analysis and numerical experiments are based on the Taylor-Hood element (P2-P1). Then, we define $\mathbf{U}_h = (\mathbf{X}_{fh} \times X_{ph}) \subset (\mathbf{X}_f \times X_p)$. Discretely, divergence-free velocities will be sought in the test space

$$\mathbf{V}_h = \left\{ \mathbf{v}_h \in \mathbf{U}_h : \int_{\Omega} q_{fh} \nabla \cdot \mathbf{v}_h d\Omega = 0, \quad \forall q_{fh} \in Q_{fh} \right\}.$$

Throughout the remainder of this paper we will use $\mathbf{tu} := (\mathbf{tu}_f, t\phi_p)$ and $tp_f, \hat{\mathbf{u}}_h := (\hat{\mathbf{u}}_f, \hat{\phi}_p)$ and \hat{p}_f , $\mathbf{cu}_h := (\mathbf{cu}_f, c\phi_p)$ and cp_f to denote the true solutions, the defect step approximations and the deferred correction step approximations, respectively.

For $t \in [0, T]$, $\hat{\mathbf{u}}_h^n$ and \mathbf{cu}_h^n will denote the discrete approximations to \mathbf{tu}^n ($n = 0, 1, \dots, N$). Artificial viscosities H_f and H_p are positive and chosen as additional parameters of the Stokes equation and the Darcy equation, respectively. For the convenience of the theoretical analysis, we let $a_\Omega((v + H)\mathbf{u}, \mathbf{v}) = a_{\Omega_f}((\nu + H_f)\mathbf{u}_f, \mathbf{v}_f) + a_{\Omega_p}((\mathbb{K} + H_p\mathbb{I})\phi_p, \psi_p)$, where H is also a symbol, and it is used to keep $a_\Omega((v + H)\mathbf{u}, \mathbf{v})$ and $a_{\Omega_f}((\nu + H_f)\mathbf{u}_f, \mathbf{v}_f)$, $a_{\Omega_p}((\mathbb{K} + H_p\mathbb{I})\phi_p, \psi_p)$ in the same structure. Moreover, in the subsequent numerical examples, we take $H_f = H_p$.

After that, we will introduce the defect-deferred correction algorithm: Given $\hat{\mathbf{u}}_h^n \in \mathbf{U}_h$, $\mathbf{cu}_h^n \in \mathbf{U}_h$, find $(\hat{\mathbf{u}}_h^{n+1}, \hat{p}_f^{n+1}) \in (\mathbf{U}_h, Q_{fh})$, $(\mathbf{cu}_h^{n+1}, cp_f^{n+1}) \in (\mathbf{U}_h, Q_{fh})$ with $n = 0, 1, 2 \dots N - 1$, for all $\mathbf{v}_h \in \mathbf{U}_h$, satisfying

$$\begin{aligned} & \left(\frac{\hat{\mathbf{u}}_h^{n+1} - \hat{\mathbf{u}}_h^n}{\Delta t}, \mathbf{v}_h \right) + a_\Omega((v + H)\hat{\mathbf{u}}_h^{n+1}, \mathbf{v}_h) + a_\Gamma(\hat{\mathbf{u}}_h^{n+1}, \mathbf{v}_h) - b(\mathbf{v}_h, \hat{p}_f^{n+1}) \\ & = \langle \mathbf{F}^{n+1}, \mathbf{v}_h \rangle_{\mathbf{U}'}, \end{aligned} \quad (3)$$

and

$$\begin{aligned} & \left(\frac{\mathbf{cu}_h^{n+1} - \mathbf{cu}_h^n}{\Delta t}, \mathbf{v}_h \right) + a_\Omega((v + H)\mathbf{cu}_h^{n+1}, \mathbf{v}_h) + a_\Gamma(\mathbf{cu}_h^{n+1}, \mathbf{v}_h) - b(\mathbf{v}_h, cp_f^{n+1}) \\ & = Ha_\Omega \left(\frac{\hat{\mathbf{u}}_h^{n+1} + \hat{\mathbf{u}}_h^n}{2}, \mathbf{v}_h \right) + \left\langle \frac{\mathbf{F}^{n+1} + \mathbf{F}^n}{2}, \mathbf{v}_h \right\rangle_{\mathbf{U}'} \\ & + a_\Gamma \left(\frac{\hat{\mathbf{u}}_h^{n+1} - \hat{\mathbf{u}}_h^n}{2}, \mathbf{v}_h \right) + a_\Omega \left((v + H) \frac{\hat{\mathbf{u}}_h^{n+1} - \hat{\mathbf{u}}_h^n}{2}, \mathbf{v}_h \right) \\ & + a_\Gamma \left(\frac{\hat{\mathbf{u}}_h^{n+1} - \hat{\mathbf{u}}_h^n}{2}, \mathbf{v}_h \right) - \frac{\Delta t}{2} b \left(\mathbf{v}_h, \frac{\hat{p}_f^{n+1} - \hat{p}_f^n}{\Delta t} \right). \end{aligned} \quad (4)$$

Here (3) is the defect step and (4) is the deferred correction step. The terms on the right-hand side of (4) are written in a form that hints at the reason for the increased accuracy of the deferred correction step solution. Note also that the matrix of the system is identical for (3) and (4) because of the similar structure on the left.

Then we consider the sensitivity of artificial viscosity in the defect-deferred correction method based on the continuous sensitivity equation method. Define $\hat{\zeta}_h = \frac{\partial \hat{\mathbf{u}}_h}{\partial H} = \left(\frac{\partial \hat{\mathbf{u}}_f}{\partial H_f}, \frac{\partial \hat{\phi}_p}{\partial H_p} \right)$, $\hat{\zeta}_f = \frac{\partial \hat{p}_f}{\partial H_f}$ and $c\hat{\zeta}_h = \frac{\partial \mathbf{cu}_h}{\partial H} = \left(\frac{\partial c\mathbf{u}_f}{\partial H_f}, \frac{\partial c\phi_p}{\partial H_p} \right)$, $c\hat{\zeta}_f = \frac{\partial cp_f}{\partial H_f}$. The derivative of the defect deferred correction method (3) and (4) for the Stokes/Darcy model with respect to artificial viscosity H results in the following system: Given $\hat{\zeta}_h^n \in \mathbf{U}_h$, $\hat{\zeta}_h^n \in \mathbf{U}_h$, find $(\hat{\zeta}_h^{n+1}, \hat{\zeta}_f^{n+1}) \in (\mathbf{U}_h, Q_{fh})$, $(c\hat{\zeta}_h^{n+1}, c\hat{\zeta}_f^{n+1}) \in (\mathbf{U}_h, Q_{fh})$ with $n = 0, 1, 2 \dots N - 1$, for all $\mathbf{v}_h \in \mathbf{U}_h$, satisfying

$$\begin{aligned} & \left(\frac{\hat{\zeta}_h^{n+1} - \hat{\zeta}_h^n}{\Delta t}, \mathbf{v}_h \right) + a_\Omega((v + H)\hat{\zeta}_h^{n+1}, \mathbf{v}_h) + a_\Omega(\hat{\mathbf{u}}_h^{n+1}, \mathbf{v}_h) + a_\Gamma(\hat{\zeta}_h^{n+1}, \mathbf{v}_h) \\ & - b(\mathbf{v}_h, \hat{\zeta}_f^{n+1}) = 0, \end{aligned} \quad (5)$$

and

$$\begin{aligned}
& \left(\frac{c\xi_h^{n+1} - c\xi_h^n}{\Delta t}, \mathbf{v}_h \right) + a_\Omega((v+H)c\xi_h^{n+1}, \mathbf{v}_h) + a_\Omega(\mathbf{c}\mathbf{u}_h^{n+1}, \mathbf{v}_h) + a_\Gamma(c\xi_h^{n+1}, \mathbf{v}_h) \\
& - b(\mathbf{v}_h, c\xi_f^{n+1}) = a_\Omega \left((v+H) \frac{\hat{\xi}_h^{n+1} - \hat{\xi}_h^n}{2}, \mathbf{v}_h \right) + a_\Omega \left(\frac{\hat{\mathbf{u}}_h^{n+1} - \hat{\mathbf{u}}_h^n}{2}, \mathbf{v}_h \right) \\
& + a_\Omega \left(\frac{\hat{\mathbf{u}}_h^{n+1} + \hat{\mathbf{u}}_h^n}{2}, \mathbf{v}_h \right) + Ha_\Omega \left(\frac{\hat{\xi}_h^{n+1} + \hat{\xi}_h^n}{2}, \mathbf{v}_h \right) + a_\Gamma \left(\frac{\hat{\xi}_h^{n+1} - \hat{\xi}_h^n}{2}, \mathbf{v}_h \right) \\
& - \frac{\Delta t}{2} b \left(\mathbf{v}_h, \frac{\hat{\xi}_f^{n+1} - \hat{\xi}_f^n}{\Delta t} \right). \tag{6}
\end{aligned}$$

4. Sensitivity analysis

In this section, we mainly establish the estimates of sensitive equations (5) and (6). At the beginning, let us first state and prove the estimates of (3) and (4).

Theorem 1 (Estimates of defect approximation). *Let $\hat{\mathbf{u}}_h^{n+1}$ with initial data $\hat{\mathbf{u}}_h^0$ satisfy (3) for each $n \in \{0, 1, 2, \dots, N-1\}$. Then we get*

$$\|\hat{\mathbf{u}}_h^N\|_0^2 + \Delta t(v+H)C_{coe} \sum_{n=0}^{N-1} \|\hat{\mathbf{u}}_h^{n+1}\|_U^2 \leq \frac{\Delta t(C_p^2 + \tilde{C}_p^2)}{C_{coe}(v+H)} \sum_{n=0}^{N-1} \|\mathbf{F}^{n+1}\|_{L^2}^2 + \|\hat{\mathbf{u}}_h^0\|_0^2. \tag{7}$$

Proof. By setting $\mathbf{v}_h = \hat{\mathbf{u}}_h^{n+1} \in \mathbf{V}_h$ in (3), we can arrive at

$$\begin{aligned}
& \left(\frac{\hat{\mathbf{u}}_h^{n+1} - \hat{\mathbf{u}}_h^n}{\Delta t}, \hat{\mathbf{u}}_h^{n+1} \right) + a_\Omega((v+H)\hat{\mathbf{u}}_h^{n+1}, \hat{\mathbf{u}}_h^{n+1}) + a_\Gamma(\hat{\mathbf{u}}_h^{n+1}, \hat{\mathbf{u}}_h^{n+1}) \\
& = \langle \mathbf{F}^{n+1}, \hat{\mathbf{u}}_h^{n+1} \rangle_{\mathbf{U}'}.
\end{aligned}$$

Thanks to the Cauchy-Schwarz and Young's inequalities, we derive

$$\begin{aligned}
& \frac{\|\hat{\mathbf{u}}_h^{n+1}\|_0^2 - \|\hat{\mathbf{u}}_h^n\|_0^2}{2\Delta t} + (v+H)C_{coe}\|\hat{\mathbf{u}}_h^{n+1}\|_U^2 \\
& \leq \frac{C_{coe}(v+H)}{2}\|\hat{\mathbf{u}}_h^{n+1}\|_U^2 + \frac{(C_p^2 + \tilde{C}_p^2)}{2C_{coe}(v+H)}\|\mathbf{F}^{n+1}\|_{L^2}^2.
\end{aligned}$$

By multiplying both sides of the last inequality by $2\Delta t$ and adding up from $n = 0$ to $N-1$, the required estimate (7) holds. \square

Theorem 2 (Analysis of the defect step of the sensitive equation). *Let $\hat{\xi}_h^{n+1}$ with initial data $\hat{\xi}_h^0$ satisfy (5) for each $n \in \{0, 1, 2, \dots, N-1\}$. Then $\exists C > 0$ is independent of $h, \Delta t$ and H such that $\hat{\xi}_h^{n+1}$ satisfies*

$$\begin{aligned}
& \|\hat{\xi}_h^N\|_0^2 + \Delta t(v+H)C_{coe} \sum_{n=0}^{N-1} \|\hat{\xi}_h^{n+1}\|_U^2 \leq C \left\{ \frac{\Delta t}{(v+H)^3} \sum_{n=0}^{N-1} \|\mathbf{F}^{n+1}\|_{L^2}^2 + \|\hat{\xi}_h^0\|_0^2 \right. \\
& \left. + \frac{1}{(v+H)^2} \|\hat{\mathbf{u}}_h^0\|_0^2 \right\}. \tag{8}
\end{aligned}$$

Proof. We take $\underline{\mathbf{v}}_h = \hat{\xi}_h^{n+1} \in \mathbf{V}_h$ in (5), and then we obtain

$$\left(\frac{\hat{\xi}_h^{n+1} - \hat{\xi}_h^n}{\Delta t}, \hat{\xi}_h^{n+1} \right) + a_\Omega((v + H)\hat{\xi}_h^{n+1}, \hat{\xi}_h^{n+1}) + a_\Omega(\hat{\mathbf{u}}_h^{n+1}, \hat{\xi}_h^{n+1}) = 0.$$

With the Cauchy-Schwarz and Young's inequalities, it is easy to get

$$\begin{aligned} & \frac{\|\hat{\xi}_h^{n+1}\|_0^2 - \|\hat{\xi}_h^n\|_0^2}{2\Delta t} + (v + H)C_{coe}\|\hat{\xi}_h^{n+1}\|_U^2 \\ & \leq \frac{C_{coe}(v + H)}{2}\|\hat{\xi}_h^{n+1}\|_U^2 + \frac{C_{con}^2}{2C_{coe}(v + H)}\|\hat{\mathbf{u}}_h^{n+1}\|_U^2. \end{aligned}$$

We multiply both sides by $2\Delta t$, sum over from $n = 0$ to $N - 1$ and combine with (7). Then we yield

$$\begin{aligned} \|\hat{\xi}_h^N\|_0^2 + \Delta t(v + H)C_{coe} \sum_{n=0}^{N-1} \|\hat{\xi}_h^{n+1}\|_U^2 & \leq \frac{\Delta t C_{con}^2 (C_p^2 + \tilde{C}_p^2)}{C_{coe}^3 (v + H)^3} \sum_{n=0}^{N-1} \|\mathbf{F}^{n+1}\|_{L^2}^2 \\ & + \frac{C_{con}^2}{C_{coe}^2 (v + H)^2} \|\hat{\mathbf{u}}_h^0\|_0^2 + \|\hat{\xi}_h^0\|_0^2. \end{aligned}$$

The desired result (8) is proved. \square

It can be obtained from Theorem 2 that the sensitivity of $\hat{\mathbf{u}}_h$ on H is mainly affected by v and H , and smaller when v and H are larger. Moreover, it should be noted that the values of v and H are too small at the same time to obtain the convergence for the numerical solution $\hat{\xi}_h^N$. These provide a reference for selecting H when solving the Stokes/Darcy model with different viscosity coefficients and hydraulic conductivity coefficients.

Next, we are ready to derive the estimation of the deferred correction equation (4) and the analysis of the sensitivity equation of the deferred correction step (6).

Theorem 3 (Estimates of deferred correction approximation). *Let \mathbf{cu}_h^{n+1} with initial data \mathbf{cu}_h^0 satisfy (4) for each $n \in \{0, 1, 2, \dots, N-1\}$. Then $\exists C > 0$ is independent of h , Δt and H such that \mathbf{cu}_h^{n+1} satisfies*

$$\begin{aligned} & \|\mathbf{cu}_h^N\|_0^2 + (v + H)\Delta t \sum_{n=0}^{N-1} C_{coe}\|\mathbf{cu}_h^{n+1}\|_U^2 \\ & \leq C \left\{ \left(\frac{1 + H^2}{(v + H)^3} + \frac{1}{v + H} \right) \Delta t \sum_{n=0}^{N-1} \|\mathbf{F}^{n+1}\|_{L^2}^2 \right. \\ & \quad \left. + \left(\frac{1 + H^2}{(v + H)^2} + 1 \right) \|\hat{\mathbf{u}}_h^0\|_0^2 + \|\mathbf{cu}_h^0\|_0^2 \right\}. \end{aligned} \quad (9)$$

Proof. Letting $\mathbf{v}_h = \mathbf{c}\mathbf{u}_h^{n+1} \in \mathbf{V}_h$ in (4) yields

$$\begin{aligned} & \left(\frac{\mathbf{c}\mathbf{u}_h^{n+1} - \mathbf{c}\mathbf{u}_h^n}{\Delta t}, \mathbf{c}\mathbf{u}_h^{n+1} \right) + a_\Omega((v+H)\mathbf{c}\mathbf{u}_h^{n+1}, \mathbf{c}\mathbf{u}_h^{n+1}) + a_\Gamma(\mathbf{c}\mathbf{u}_h^{n+1}, \mathbf{c}\mathbf{u}_h^{n+1}) \\ &= \left\langle \frac{\mathbf{F}^{n+1} + \mathbf{F}^n}{2}, \mathbf{c}\mathbf{u}_h^{n+1} \right\rangle_{\mathbf{U}'} + Ha_\Omega \left(\frac{\hat{\mathbf{u}}_h^{n+1} + \hat{\mathbf{u}}_h^n}{2}, \mathbf{c}\mathbf{u}_h^{n+1} \right) \\ & \quad + a_\Gamma \left(\frac{\hat{\mathbf{u}}_h^{n+1} - \hat{\mathbf{u}}_h^n}{2}, \mathbf{c}\mathbf{u}_h^{n+1} \right) + a_\Omega \left((v+H) \frac{\hat{\mathbf{u}}_h^{n+1} - \hat{\mathbf{u}}_h^n}{2}, \mathbf{c}\mathbf{u}_h^{n+1} \right). \end{aligned} \quad (10)$$

Applying the Cauchy-Schwarz and Young's inequalities, the terms on the right-hand side in (10) can be bounded as follows:

$$\begin{aligned} \left\langle \frac{\mathbf{F}^{n+1} + \mathbf{F}^n}{2}, \mathbf{c}\mathbf{u}_h^{n+1} \right\rangle_{\mathbf{U}'} &\leq \epsilon C_{coe}(v+H) \|\mathbf{c}\mathbf{u}_h^{n+1}\|_{\mathbf{U}}^2 \\ & \quad + \frac{(C_p^2 + \tilde{C}_p^2)}{4\epsilon C_{coe}(v+H)} \left\| \frac{\mathbf{F}^{n+1} + \mathbf{F}^n}{2} \right\|_{L^2}^2, \\ Ha_\Omega \left(\frac{\hat{\mathbf{u}}_h^{n+1} + \hat{\mathbf{u}}_h^n}{2}, \mathbf{c}\mathbf{u}_h^{n+1} \right) &\leq 2\epsilon(v+H)C_{coe} \|\mathbf{c}\mathbf{u}_h^{n+1}\|_{\mathbf{U}}^2 \\ & \quad + \frac{H^2 C_{con}^2}{16\epsilon C_{coe}(v+H)} (\|\hat{\mathbf{u}}_h^{n+1}\|_{\mathbf{U}}^2 + \|\hat{\mathbf{u}}_h^n\|_{\mathbf{U}}^2), \end{aligned}$$

and

$$\begin{aligned} a_\Omega \left((v+H) \frac{\hat{\mathbf{u}}_h^{n+1} - \hat{\mathbf{u}}_h^n}{2}, \mathbf{c}\mathbf{u}_h^{n+1} \right) &\leq 2\epsilon(v+H)C_{coe} \|\mathbf{c}\mathbf{u}_h^{n+1}\|_{\mathbf{U}}^2 \\ & \quad + \frac{(v+H)C_{con}^2}{16\epsilon C_{coe}} (\|\hat{\mathbf{u}}_h^{n+1}\|_{\mathbf{U}}^2 + \|\hat{\mathbf{u}}_h^n\|_{\mathbf{U}}^2), \\ a_\Gamma \left(\frac{\hat{\mathbf{u}}_h^{n+1} - \hat{\mathbf{u}}_h^n}{2}, \mathbf{c}\mathbf{u}_h^{n+1} \right) &\leq 2\epsilon(v+H)C_{coe} \|\mathbf{c}\mathbf{u}_h^{n+1}\|_{\mathbf{U}}^2 \\ & \quad + \frac{C_\Gamma^2}{16\epsilon(v+H)C_{coe}} (\|\hat{\mathbf{u}}_h^{n+1}\|_{\mathbf{U}}^2 + \|\hat{\mathbf{u}}_h^n\|_{\mathbf{U}}^2). \end{aligned}$$

By choosing $\epsilon = \frac{1}{14}$, multiplying both sides by $2\Delta t$ and combining the above estimates, we have:

$$\begin{aligned} & \|\mathbf{c}\mathbf{u}_h^{n+1}\|_0^2 - \|\mathbf{c}\mathbf{u}_h^n\|_0^2 + \Delta t(v+H)C_{coe} \|\mathbf{c}\mathbf{u}_h^{n+1}\|_{\mathbf{U}}^2 \\ & \leq \frac{7(C_p^2 + \tilde{C}_p^2)\Delta t}{C_{coe}(v+H)} \left\| \frac{\mathbf{F}^{n+1} + \mathbf{F}^n}{2} \right\|_{L^2}^2 + \frac{7H^2 C_{con}^2 \Delta t}{4(v+H)C_{coe}} (\|\hat{\mathbf{u}}_h^{n+1}\|_{\mathbf{U}}^2 + \|\hat{\mathbf{u}}_h^n\|_{\mathbf{U}}^2) \\ & \quad + \frac{7C_\Gamma^2 \Delta t}{4(v+H)C_{coe}} (\|\hat{\mathbf{u}}_h^{n+1}\|_{\mathbf{U}}^2 + \|\hat{\mathbf{u}}_h^n\|_{\mathbf{U}}^2) + \frac{7(v+H)C_{con}^2 \Delta t}{4C_{coe}} (\|\hat{\mathbf{u}}_h^{n+1}\|_{\mathbf{U}}^2 + \|\hat{\mathbf{u}}_h^n\|_{\mathbf{U}}^2). \end{aligned}$$

Therefore, adding up from $n = 0$ to $N - 1$ and combining with (7) we get (9). \square

Theorem 4 (Analysis of the deferred correction step of the sensitive equation). *Let $c\xi_h^{n+1}$ with initial data $c\xi_h^0$ satisfy (5) for each $n \in \{0, 1, 2, \dots, N-1\}$. Then $\exists C > 0$ is independent of $h, \Delta t$ and H such that $c\xi_h^{n+1}$ satisfies*

$$\begin{aligned} & \|c\xi_h^N\|_0^2 + (v+H)\Delta t \sum_{n=0}^{N-1} C_{coe} \|c\xi_h^{n+1}\|_U^2 \\ & \leq C \left\{ \left(\frac{1+H^2}{(v+H)^5} + \frac{1}{(v+H)^3} \right) \Delta t \sum_{n=0}^{N-1} \|\mathbf{F}^{n+1}\|_{L^2}^2 \right. \\ & \quad + \left(\frac{1}{(v+H)^2} + \frac{H^2}{(v+H)^5} + \frac{1+H^2}{(v+H)^4} \right) \|\hat{\mathbf{u}}_h^0\|_0^2 + \left(1 + \frac{H^2}{(v+H)^2} \right) \|\hat{\xi}_h^0\|_0^2 \\ & \quad \left. + \frac{1}{(v+H)^2} \|\mathbf{c}\mathbf{u}_h^0\|_0^2 \right\}. \end{aligned} \quad (11)$$

Proof. Setting $\mathbf{v}_h = c\xi_h^{n+1} \in \mathbf{V}_h$ into (6), we can write it as follows:

$$\begin{aligned} & \left(\frac{c\xi_h^{n+1} - c\xi_h^n}{\Delta t}, c\xi_h^{n+1} \right) + a_\Omega((v+H)c\xi_h^{n+1}, c\xi_h^{n+1}) + a_\Omega(\mathbf{c}\mathbf{u}_h^{n+1}, c\xi_h^{n+1}) \\ & + a_\Gamma(c\xi_h^{n+1}, c\xi_h^{n+1}) = Ha_\Omega \left(\frac{\hat{\xi}_h^{n+1} + \hat{\xi}_h^n}{2}, c\xi_h^{n+1} \right) + a_\Omega \left(\frac{\hat{\mathbf{u}}_h^{n+1} + \hat{\mathbf{u}}_h^n}{2}, c\xi_h^{n+1} \right) \\ & + a_\Gamma \left(\frac{\hat{\xi}_h^{n+1} - \hat{\xi}_h^n}{2}, c\xi_h^{n+1} \right) + a_\Omega \left((v+H) \frac{\hat{\xi}_h^{n+1} - \hat{\xi}_h^n}{2}, c\xi_h^{n+1} \right) \\ & + a_\Omega \left(\frac{\hat{\mathbf{u}}_h^{n+1} - \hat{\mathbf{u}}_h^n}{2}, c\xi_h^{n+1} \right). \end{aligned} \quad (12)$$

We have the following estimates for the terms on the right-hand side in (12) by the Cauchy-Schwarz and Young's inequalities:

$$\begin{aligned} & Ha_\Omega \left(\frac{\hat{\xi}_h^{n+1} + \hat{\xi}_h^n}{2}, c\xi_h^{n+1} \right) \leq 2\epsilon(v+H)C_{coe} \|c\xi_h^{n+1}\|_U^2 \\ & \quad + \frac{H^2 C_{con}^2}{16\epsilon C_{coe} (v+H)} (\|\hat{\xi}_h^{n+1}\|_U^2 + \|\hat{\xi}_h^n\|_U^2), \\ & a_\Omega \left((v+H) \frac{\hat{\xi}_h^{n+1} - \hat{\xi}_h^n}{2}, c\xi_h^{n+1} \right) \leq 2\epsilon(v+H)C_{coe} \|c\xi_h^{n+1}\|_U^2 \\ & \quad + \frac{(v+H)C_{con}^2}{16\epsilon C_{coe}} (\|\hat{\xi}_h^{n+1}\|_U^2 + \|\hat{\xi}_h^n\|_U^2), \\ & a_\Gamma \left(\frac{\hat{\xi}_h^{n+1} - \hat{\xi}_h^n}{2}, c\xi_h^{n+1} \right) \leq 2\epsilon(v+H)C_{coe} \|c\xi_h^{n+1}\|_U^2 \\ & \quad + \frac{C_\Gamma^2}{16\epsilon(v+H)C_{coe}} (\|\hat{\xi}_h^{n+1}\|_U^2 + \|\hat{\xi}_h^n\|_U^2). \end{aligned}$$

Besides,

$$\begin{aligned} & a_{\Omega} \left(\frac{\hat{\mathbf{u}}_h^{n+1} + \hat{\mathbf{u}}_h^n}{2}, c\xi_h^{n+1} \right) + a_{\Omega} \left(\frac{\hat{\mathbf{u}}_h^{n+1} - \hat{\mathbf{u}}_h^n}{2}, c\xi_h^{n+1} \right) \\ & \leq 4\epsilon(v + H)C_{coe} \|c\xi_h^{n+1}\|_{\mathbb{U}}^2 + \frac{C_{con}^2}{8\epsilon(v + H)C_{coe}} (\|\hat{\mathbf{u}}_h^{n+1}\|_{\mathbb{U}}^2 + \|\hat{\mathbf{u}}_h^n\|_{\mathbb{U}}^2), \end{aligned}$$

and

$$a_{\Omega}(\mathbf{cu}_h^{n+1}, c\xi_h^{n+1}) \leq \epsilon(v + H)C_{coe} \|c\xi_h^{n+1}\|_{\mathbb{U}}^2 + \frac{C_{con}^2}{4\epsilon C_{coe}(v + H)} \|\mathbf{cu}_h^{n+1}\|_{\mathbb{U}}^2.$$

The required estimate (11) now follows by choosing $\epsilon = \frac{1}{22}$, multiplying both sides by $2\Delta t$, adding up from $n = 0$ to $N - 1$, and combining Theorem 1, Theorem 2 and Theorem 3. \square

From Theorem 4, we can see that the sensitivity of \mathbf{cu}_h on H is mainly affected by v and H . On the one hand, when H is selected, v is larger, the sensitivity of \mathbf{cu}_h on H is smaller. On the other hand, when v is selected, the sensitivity of \mathbf{cu}_h on H is weaker when H is much greater or smaller than v compared with taking three adjacent values. Similarly, v and H should not be too small here, otherwise the numerical solution will also be divergent. According to the sensitivity of \mathbf{cu}_h on H affected by v and H , we can choose the appropriate H to solve more efficiently the Stokes/Darcy problems with different viscosity coefficients and hydraulic conductivity coefficients.

5. Numerical experiments

In this section, some numerical experiments will be carried out to verify theoretical analysis results obtained in the previous sections on the sensitivity analysis of the defect-deferred correction method of the non-stationary coupled Stokes/Darcy model using the continuous sensitivity equation method. Furthermore, we implemented the code using the software package FreeFEM++ [15].

5.1. An analytical solution problem

In these experiments, for different values of v , we study the effect of H on the sensitivity of $\hat{\mathbf{u}}_f$ and $\hat{\phi}_p$. All physical parameters ρ, g, α, S are simply set to 1. The final time is chosen as $T = 1$. The space step and the time step are taken as $\frac{1}{50}$. We assume the area as $\Omega_f = [0, 1] \times [1, 2]$, $\Omega_p = [0, 1] \times [0, 1]$, $\Gamma = (0, 1) \times \{1\}$ and give the analytical solution:

$$\begin{aligned} \mathbf{u}_f &= \left((x^2(y-1)^2 + y)\cos(t), -\frac{2}{3}x(y-1)^3\cos(t) + (2 - \pi\sin(\pi x))\cos(t) \right), \\ p_f &= (2 - \pi\sin(\pi x))\sin(0.5\pi y)\cos(t), \\ \phi_p &= (2 - \pi\sin(\pi x))(1 - y - \cos(\pi y))\cos(t). \end{aligned}$$

H_f	1.0E-1	1.0E-2	1.0E-3	1.0E-4	1.0E-5
$\nu = 1.0E-0$	3.93E-2	4.78E-2	4.87E-2	4.88E-2	4.89E-2
$\nu = 1.0E-1$	1.45E-1	3.71E-1	4.34E-1	4.41E-1	4.42E-1
$\nu = 1.0E-2$	7.61E-1	2.69E-0	5.54E-0	6.09E-0	6.15E-0
$\nu = 1.0E-3$	9.02E-1	5.07E-0	—	—	—
$\nu = 1.0E-4$	9.17E-1	5.55E-0	—	—	—
$\nu = 1.0E-5$	9.19E-1	5.60E-0	—	—	—

Table 1: The values of $\|\frac{\partial \hat{\mathbf{u}}_f}{\partial H_f}\|_0$ in the sensitive equation of the defect step

H_p	1.0E-1	1.0E-2	1.0E-3	1.0E-4	1.0E-5
$\mathbb{K} = 1.0E-0\mathbb{I}$	5.59E-1	6.60E-1	6.72E-1	6.73E-1	6.73E-1
$\mathbb{K} = 1.0E-1\mathbb{I}$	1.98E-0	4.97E-0	5.49E-0	5.55E-0	5.55E-0
$\mathbb{K} = 1.0E-2\mathbb{I}$	2.82E-0	1.20E+1	1.45E+1	1.48E+1	1.48E+1
$\mathbb{K} = 1.0E-3\mathbb{I}$	2.99E-0	1.41E+1	—	—	—
$\mathbb{K} = 1.0E-4\mathbb{I}$	3.01E-0	1.44E+1	—	—	—
$\mathbb{K} = 1.0E-5\mathbb{I}$	3.01E-0	1.45E+1	—	—	—

Table 2: The values of $\|\frac{\partial \hat{\phi}_p}{\partial H_p}\|_0$ in the sensitive equation of the defect step

Table 1 and Table 2 show the values of $\|\frac{\partial \hat{\mathbf{u}}_f}{\partial H_f}\|_0$ at different values of ν and H_f , and the value of $\|\frac{\partial \hat{\phi}_p}{\partial H_p}\|_0$ at different values of \mathbb{K} and H_p in the sensitivity equations of the defect step (5), respectively. Based on these data, we can observe that the larger values of ν , \mathbb{K} , H_f and H_p , the smaller the sensitivity of $\hat{\mathbf{u}}_h$ on H and vice versa. Furthermore, if the values of H_f , H_p , ν and \mathbb{K} are all less than 0.01, the equations (5) cannot be solved, which will result such that the numerical solution of the equations (3) cannot be obtained. It is obvious that it agrees with the theoretical results.

H_f	1.0E-1	1.0E-2	1.0E-3	1.0E-4	1.0E-5
$\nu = 1.0E-0$	7.83E-3	4.93E-4	5.74E-4	6.76E-4	6.86E-4
$\nu = 1.0E-1$	1.33E-1	1.03E-1	1.21E-2	1.01E-2	1.02E-2
$\nu = 1.0E-2$	7.43E-1	2.19E-0	6.52E-1	1.92E-1	2.08E-1
$\nu = 1.0E-3$	8.80E-1	6.66E-0	—	—	—
$\nu = 1.0E-4$	8.95E-1	7.83E-0	—	—	—
$\nu = 1.0E-5$	8.96E-1	7.97E-0	—	—	—

Table 3: The values of $\|\frac{\partial \mathbf{cu}_f}{\partial H_f}\|_0$ of the sensitive equation of the deferred correction step

From Table 3 and Table 4, on the one hand, we can find that the sensitivity of \mathbf{cu}_h on H is weaker when H_f and H_p are taken, and ν and \mathbb{K} are larger. Moreover, when ν and \mathbb{K} are taken, the sensitivity of \mathbf{cu}_h on H is weaker when H_f and H_p is much greater or smaller than ν and \mathbb{K} compared with taking three adjacent values. In addition, we can also see that if ν , \mathbb{K} , H_f and H_p are all less than 0.01, sensitivity equations (6) cannot be solved which causes that we are unable to calculate the equations (4). These conclusions above coincide apparently with our theoretical results.

H_p	1.0E-1	1.0E-2	1.0E-3	1.0E-4	1.0E-5
$\mathbb{K} = 1.0\text{E-}0\text{II}$	1.06E-1	6.86E-3	6.48E-3	7.85E-3	7.99E-3
$\mathbb{K} = 1.0\text{E-}1\text{II}$	2.03E-0	5.93E-1	4.81E-2	1.79E-2	2.38E-2
$\mathbb{K} = 1.0\text{E-}2\text{II}$	4.50E-0	2.81E-0	4.64E-1	1.48E-1	1.46E-1
$\mathbb{K} = 1.0\text{E-}3\text{II}$	5.03E-0	4.59E-0	—	—	—
$\mathbb{K} = 1.0\text{E-}4\text{II}$	5.08E-0	4.97E-0	—	—	—
$\mathbb{K} = 1.0\text{E-}5\text{II}$	5.09E-0	5.02E-0	—	—	—

Table 4: The values of $\|\frac{\partial c\phi_p}{\partial H_p}\|_0$ of the sensitive equation of the deferred correction step

5.2. Other exact solution problem

In order to further verify our conclusion, we additionally select another exact solution. Physical parameters ρ, g, α, S are simply set to 1. ν and the space step h are varied. The final time is $T = 1$. The time step is taken as $\frac{1}{50}$. We assume the area as $\Omega_f = [0, 1] \times [1, 2]$, $\Omega_p = [0, 1] \times [0, 1]$, $\Gamma = (0, 1) \times \{1\}$ and give the analytical solution:

$$\begin{aligned} \mathbf{u}_f &= \left(\frac{K_{11}}{\pi} \sin(2\pi y) \cos(x) e^t, (-2K_{22} + \frac{K_{22}}{\pi^2} \sin^2(\pi y)) \sin(x) e^t \right), \\ p &= 0, \\ \phi &= (e^y - e^{-y}) \sin(x) e^t. \end{aligned}$$

In this part of the experiment, we study the effects of ν, h , and H on the sensitivity of $\hat{\mathbf{u}}_f, \hat{\phi}_p, \mathbf{c}\mathbf{u}_f$ and $c\phi_p$. Below we will give four groups of figures. Each group of figures contains three pictures, representing the sensitivity analysis of $\hat{\mathbf{u}}_f, \hat{\phi}_p, \mathbf{c}\mathbf{u}_f$ and $c\phi_p$ under different spatial step sizes h, H_f and H_p , when ν and \mathbb{K} take 1, 0.1 and 0.01, respectively.

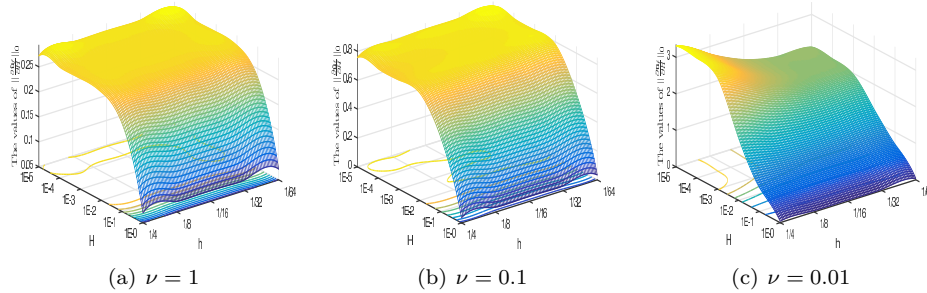


Figure 1: The values of $\|\frac{\partial \hat{\mathbf{u}}_f}{\partial H_f}\|_0$ under different ν

Figure 1 and Figure 2 indicate that when H_f and H_p are given, the bigger values of ν and \mathbb{K} , the smaller sensitivity of $\hat{\mathbf{u}}_h$ on H . Meanwhile, from (a), (b) and (c) in Figure 1 and Figure 2, we can observe that when ν and \mathbb{K} are selected, the values of H_f and H_p are large, the sensitivity of $\hat{\mathbf{u}}_h$ on H is weak. Additionally, the selection of spatial step size has little effect on the sensitivity of $\hat{\mathbf{u}}_h$ on H .

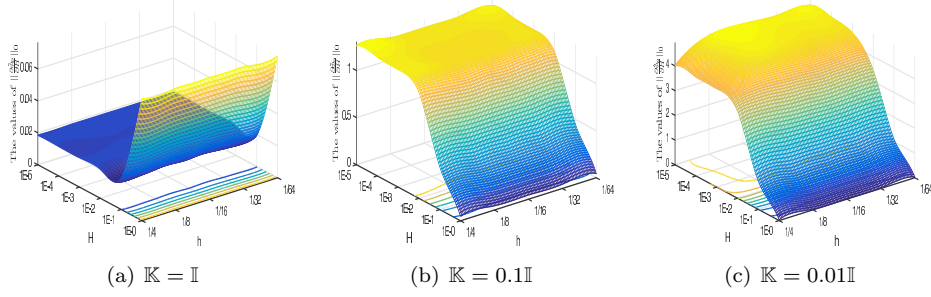


Figure 2: The values of $\|\frac{\partial \hat{\phi}}{\partial H_p}\|_0$ under different \mathbb{K}

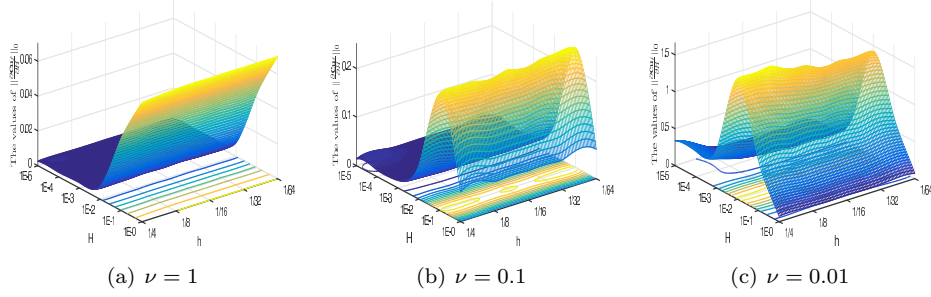


Figure 3: The values of $\|\frac{\partial \mathbf{c}u_f}{\partial H_f}\|_0$ under different ν

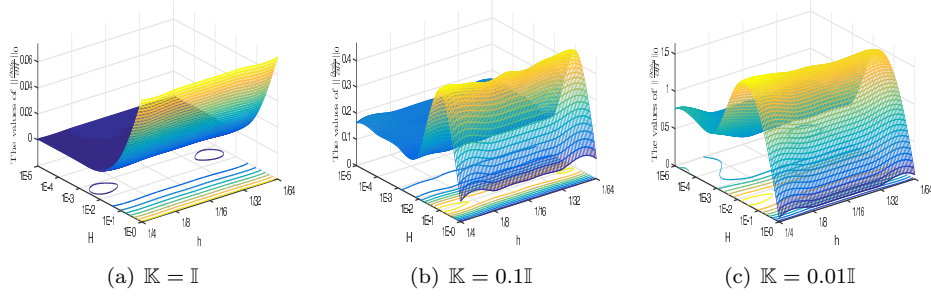


Figure 4: The values of $\|\frac{\partial \mathbf{c}\hat{\phi}}{\partial H_p}\|_0$ under different \mathbb{K}

From Figure 3 and Figure 4, it can be clearly seen that when H_f and H_p are fixed, as ν and \mathbb{K} enhance, the sensitivity of $\mathbf{c}u_h$ on H significantly decrease. Looking transversely at the three graphs in figures 3 and 4, ν and \mathbb{K} are given, and the sensitivity of $\mathbf{c}u_h$ on H is stronger when H_f , H_p and ν , \mathbb{K} have similar values than them have one dominant side. Specifically, while $\nu = H_f$ and $\mathbb{K} = H_p\mathbb{I}$, the

sensitivity of \mathbf{cu}_h on H will reach a peak.

Acknowledgement

This work was supported by the Natural Science Foundation of China (grant number 11861067), the Natural Science Foundation of Xinjiang Uygur Autonomous Region (grant number 2021D01E11) and the Xinjiang Key Laboratory of Applied Mathematics (grant number XJDX1401). We would like to express our sincere gratitude to the editor and anonymous reviewers for their helpful suggestions on the quality improvement of our present paper.

References

- [1] M. ANITESCU, W. J. LAYTON, *Sensitivities in large eddy simulation and improved estimates of turbulent flow functionals*, J. Comput. Phys. **178**(2001), 391–426.
- [2] M. AGGUL, J. M. CONNORS, D. ERKMEN, A. E. LABOVSKY, *A defect-deferred correction method for fluid-fluid interaction*, SIAM J. Numer. Anal. **56**(2018), 2484–2512.
- [3] M. AGGUL, A. LABOVSKY, *A high accuracy minimally invasive regularization technique for Navier-Stokes equations at high Reynolds number*, Numer. Meth. Part. Differ. Equ. **33**(2016), 814–839.
- [4] T. ARBOGAST, D. S. BRUNSON, *A computational method for approximating a Darcy-Stokes system governing a vuggy porous medium*, Comput. Geosci. **11**(2007), 207–218.
- [5] J. BORGGGAARD, J. BURNS, *A PDE sensitivity equation method for optimal aerodynamic design*, J. Comput. Phys. **136**(1997), 366–384.
- [6] J. BORGGGAARD, A. VERMA, *On efficient solutions to continuous sensitivity equations using automatic differentiation*, SIAM J. Sci. Comput. **22**(2001), 39–62.
- [7] L. BADEA, M. DISCACCIATI, A. QUARTERONI, *Numerical analysis of the Navier-Stokes/Darcy coupling*, Numer. Math. **115**(2010), 195–227.
- [8] M.C. CAI, M. MU, J.C. XU, *Numerical solution to a mixed Navier-Stokes/Darcy model by the two-grid approach*, SIAM J. Numer. Anal. **47**(2009), 3325–3338.
- [9] G. S. BEAVERS, D. D. JOSEPH, *Boundary conditions at a naturally permeable wall*, J. Fluid Mech. **30**(1967), 197–207.
- [10] W. CHEN, M. GUNZBURGER, D. SUN, *Efficient and long-time accurate second-order methods for Stokes-Darcy system*, SIAM J. Numer. Anal. **51**(2012), 493–497.
- [11] J. CONNORS, J. HOWELL, W. LAYTON, *Partitioned timestepping for a parabolic two domain problem*, SIAM J. Numer. Anal. **47**(2009), 3526–3549.
- [12] M. DISCACCIATI, E. MIGLIO, A. QUARTERONI, *Mathematical and numerical models for coupling surface and groundwater flows*, Appl. Numer. Math. **43**(2002), 57–74.
- [13] D. ERKMEN, A. E. LABOVSKY, *Defect-deferred correction method for the two-domain convection-dominated convection-diffusion problem*, J. Math. Anal. Appl. **450**(2017), 180–196.
- [14] M. GUNZBURGER, *Sensitivities, adjoints and flow optimization*, Int. J. Numer. Meth. Fluids. **31**(1999), 53–78.
- [15] F. HECHT, *New development in FreeFem++*, J. Numer. Math. **20**(2012), 251–265.
- [16] W. JÄGER, A. MIKELIĆ, *On the interface boundary condition of Beavers, Joseph, and Saffman*, SIAM J. Numer. Anal. **60**(2000) 1111–1127.
- [17] I. P. JONES, *Low Reynolds number flow past a porous spherical shell*, Proc. Camb. Phil. Soc. **73**(1973), 231–238.

- [18] W. LAYTON, C. TRENCH, *Stability of two IMEX methods, CNLF and BDF2-AB2, for uncoupling systems of evolution equations*, Appl. Numer. Math. **62**(2012), 112–120.
- [19] W. LAYTON, H. TRAN, C. TRENCH, *Analysis of long time stability and errors of two partitioned methods for uncoupling evolutionary groundwater-surface water flows*, SIAM J. Numer. Anal. **51**(2013), 248–272.
- [20] X. Z. LI, P. Z. HUANG, *A sensitivity study of relaxation parameter in Uzawa algorithm for the steady natural convection model*, Int. J. Numer. Methods Heat Fluid Flow **30**(2020), 818–833.
- [21] W. LI, J. FANG, Y. QIN, P. HUANG, *Rotational pressure-correction method for the Stokes/Darcy model based on the modular grad-div stabilization*, Appl. Numer. Math. **160**(2021), 451–465.
- [22] K. A. MARDAL, X. C. TAI, *A robust finite element method for Darcy–Stokes flow*, SIAM J. Numer. Anal. **40**(2002), 1605–1631.
- [23] M. MU, J. XU, *A two-grid method of a mixed Stokes-Darcy model for coupling fluid flow with porous media flow*, SIAM J. Numer. Anal. **45**(2007), 1801–1813.
- [24] V. NASSEHI, *Modelling of combined Navier-Stokes and Darcy flows in crossflow membrane filtration*, Chem. Eng. Sci. **53**(1998), 1253–1265.
- [25] M. NEDA, F. PAHLEVANI, L. G. REBHOLZ, J. WATERS, *Sensitivity analysis of the grad-div stabilization parameter in finite element simulations of incompressible flow*, J. Numer. Math. **24**(2016), 189–206.
- [26] F. PAHLEVANI, *Sensitivity computations of eddy viscosity models with an application in drag computation*, Int. J. Numer. Meth. Fluids. **52**(2006), 381–392.
- [27] Y. QIN, Y. R. HOU, *The time filter for the non-stationary coupled Stokes/Darcy model*, Appl. Numer. Math. **146**(2019), 260–275.
- [28] Y. QIN, Y. R. HOU, P. HUANG, Y. S. WANG, *Numerical analysis of two grad-div stabilization methods for the time-dependent Stokes/Darcy model*, Comput. Math. Appl. **79**(2020), 817–832.
- [29] B. RIVIÉRE, *Analysis of a discontinuous finite element method for the coupled Stokes and Darcy problems*, J. Sci. Comput. **22-23**(2005), 479–500.
- [30] P. SAFFMAN, *On the boundary condition at the surface of a porous medium*, Stud. Appl. Math **50**(1971), 93–101.
- [31] B. SANTIAGO, R. CODINA, *Unified stabilized finite element formulations for the Stokes and the Darcy problems*, SIAM J. Numer. Anal. **47**(2009), 1971–2000.
- [32] E. TURGEON, D. PELLETIER, J. BORGGAARD, *Applications of continuous sensitivity equations to flows with temperature dependent properties*, Numer. Heat Tr. A. **44**(2003), 611–624.